Radiative/EW penguin decays at Belle

Nanae Taniguchi (for the Belle Collaboration)
KEK-IPNS, Institute of Nuclear and Particle Studies, High Energy Accelerator Research Organization

Abstract. We present recent results for radiative and electroweak penguin decays of B meson at Belle. Measurements of differential branching fraction, isospin asymmetry, K^* polarization, and forward-backward asymmetry as functions of q^2 for $B \to K^{(*)}ll$ decays are reported. For the results of the radiative process, we report measurements of branching fractions for inclusive $B \to X_s\gamma$ and the exclusive $B \to K\eta'\gamma$ modes.

1. Introduction

$b \to s$ transition is the Flavor changing neutral currents (FCNC) which are forbidden at the tree level in the Standard Model. However, loop-induced FCNC (called penguin decays) are possible. New particles in the loops can give effects at the same order as Standard Model contributions. The process is a sensitive probe to new physics.

2. Analysis techniques

B-factory provide large clear sample of $\Upsilon(4S)$ decays $B\bar{B}$ pairs. The main background source comes from continuum events ($e^+e^- \to q\bar{q}(\gamma)$, $q = u, d, s, c$). To suppress the continuum background, we use a selection criteria making use of the difference of the event topology between B decays and continuum events. In the inclusive analysis, these continuum backgrounds are subtracted using the off-resonance data sample taken slightly below the $\Upsilon(4S)$ resonance. In the exclusive measurements, one can require the kinematic constraints on the beam-energy constrained mass $M_{\rm bc} = \sqrt{E^*_{\rm beam} - p^*_B}$ and $\Delta E = E^*_B - E^*_{\rm beam}$, using the beam energy $E^*_{\rm beam}$ and momentum p^*_B and E^*_B of B candidate in the center-of-mass system (c.m.s).

3. $B \to K^{(*)}ll$

The decay $b \to sll$ is induced through penguin or box diagrams at lower order[1]. There are many observable such as branching fraction, isospin asymmetry and forward-backward asymmetry where new physics can contribute. These observable can be interpreted in term of Wilson coefficients. Three Wilson coefficients, $C_{7,9,10}$ contribute. The B($B \to X_s\gamma$) can constraint to $|C_7|$. The $b \to sll$ is sensitive to sign of C_7.

We have measured $b \to sll$ exclusively ($B \to K^{(*)}ll$) on 657M $B\bar{B}$ pairs [2]. 10 final state ($K^+\pi^-, K_s\pi^+, K^+\pi^0, K^+$ and Ks) are reconstructed for $K^{(*)}$ and combined with electron and muon pairs. B meson is exclusively reconstructed with $M_{\rm bc}$ and ΔE. Main backgrounds are continuum event and semi-leptonic B decays. The continuum background is suppressed using information of event topology and the semi-leptonic B decays are suppressed using information of missing mass and lepton vertex separation. Dominant peaking background from $B \to J/\psi(\to ll)X$ and $\psi(2S)(\to ll)X$ decays are rejected in the q^2(invariant mass of dilepton).

We obtain $\mathcal{B}(B \to K^*ll) = (10.8 \pm 1.0 \pm 0.9) \times 10^{-7}$ and $\mathcal{B}(B \to Kll) = (4.8^{+0.5}_{-0.4} \pm 0.9) \times 10^{-7}$ by fitting to $M_{\rm bc}$ (and $M_{K\pi}$ for K^*ll). Fig. 1 shows the distributions of $M_{K\pi}$ ($M_{\rm bc}$) with fit results superimposed for the event in the $M_{\rm bc}$ ($M_{K\pi}$) signal region.

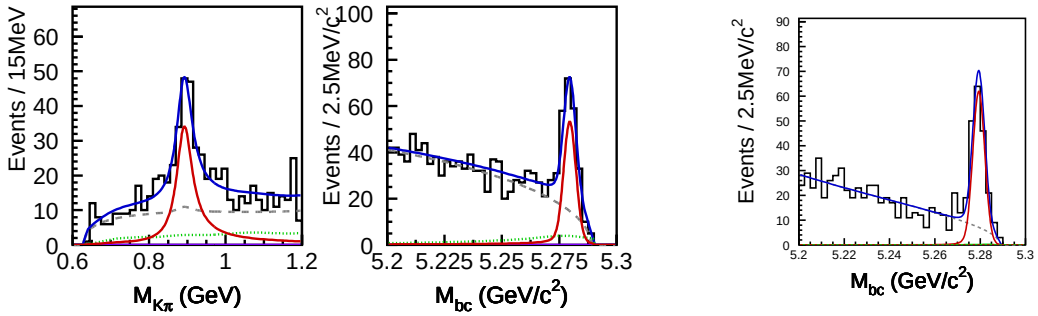

Figure 1. Distributions of $M_{K\pi}$ ($M_{\rm bc}$) with fit results superimposed for the events in the $M_{\rm bc}$ ($M_{K\pi}$) signal region. The solid curves, solid peak, dashed curves, and dotted curves represent the combined fit result, fitted signal, combinatorial background, and $J/\psi(\psi')X$ background, respectively.

We divide q^2 into 6 bins and extract the signal and combinatorial background yield in each bin. The K^* longitudinal polarization fractions (F_L) and the forward-backward asymmetry (A_{FB}) are extracted from fits in the signal region to $\cos\theta_{K^*}$ and $\cos\theta_{Bl}$, respectively, where θ_{K^*} is the angle between the kaon direction and the direction opposite the B meson in the K^* rest frame, and θ_{Bl} is the angle between the $l^+(l^-)$ and the opposite of the $B(\bar{B})$ direction in the dilepton rest frame. The differential branching fraction, F_L, and A_{FB} as functions of q^2 for $K^*\ell^+\ell^-$ and $K\ell^+\ell^-$ modes are shown in Fig. 2, Fig. 3, and Fig. 4, respectively. The differential branching fraction and F_L are consistent with the Standard Model predictions. The $A_{FB}(q^2)$ spectrum, although consistent with previous measurements [5], tends to be shifted toward the positive side from the SM expectation. A much larger data is needed for more precise measurement. Isospin

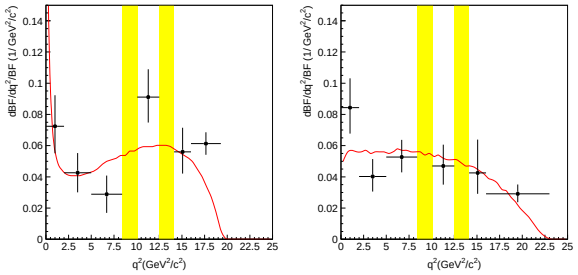

Figure 2. Differential branching fractions for $K^*\ell^+\ell^-$ (left) and $K\ell^+\ell^-$ (right) modes as a function of q^2. The two shaded regions are veto windows to reject $J/\psi(\psi')X$ events. The solid curve is the theoretical prediction [3].

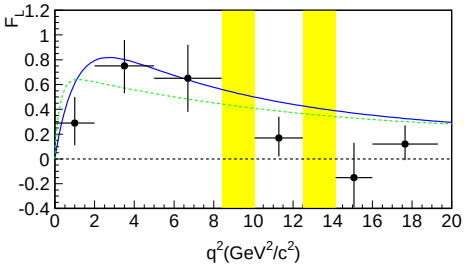

Figure 3. Fit results for F_L as a function of q^2. The solid (dashed) curve shows the SM ($C_7 = -C_7^{SM}$) prediction.

asymmetry(A_I) is shown in Fig. 5. In the Standard Model, A_I is expected to be small. Babar found a large negative asymmetry in the low q^2 region [4], however no significant asymmetry is found in Belle data.

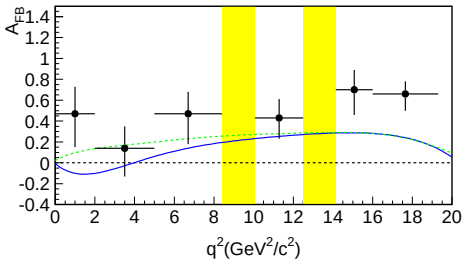

Figure 4. Fit results for A_{FB} as a function of q^2. The solid (dashed) curve shows the SM ($C_7 = -C_7^{SM}$) prediction.

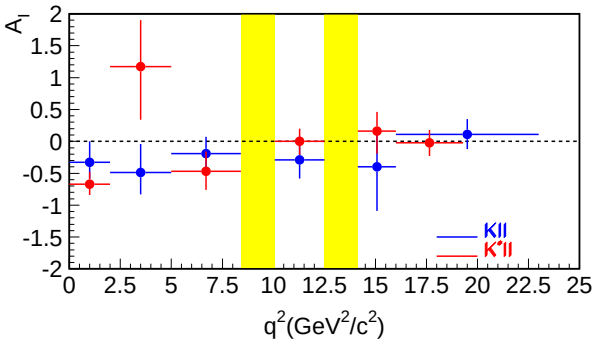

Figure 5. A_I as a function of q^2 for $K^*\ell^+\ell^-$ (red) and $K\ell^+\ell^-$ (blue) modes.

4. $b \to s\gamma$

The decay $b \to s\gamma$ is induced through penguin diagrams. The high energy real photon is an excellent experimental signature of the fully inclusive measurement.

4.1. Inclusive $B \to X_s\gamma$

The $\mathcal{B}(B \to X_s\gamma)$ have been measured in fully inclusive method [6]. We collect all high-energy photons, vetoing those originating from π^0 and η decays two photons, in calorimeter. The continuum background is suppressed using event topology information and reminder is subtracted. We estimate the contribution from continuum event using off-resonance data. The events from B decays are estimated using MC sample which calibrated with control data sample. Fig. 6 show the extracted photon energy spectrum. We obtain $\mathcal{B}(B \to X_s\gamma) = (3.31 \pm 0.19 \pm 0.37 \pm 0.01) \times 10^{-4}$, $\langle E_\gamma \rangle = 2.281 \pm 0.032 \pm 0.053 \pm 0.002$ GeV, $\langle E_\gamma^2 \rangle - \langle E_\gamma \rangle^2 = 0.0396 \pm 0.0156 \pm 0.0214 \pm 0.0012$ GeV^2 for $E_\gamma^{c.m.s} > 1.7$ GeV. These results are the most precise measurements to date.

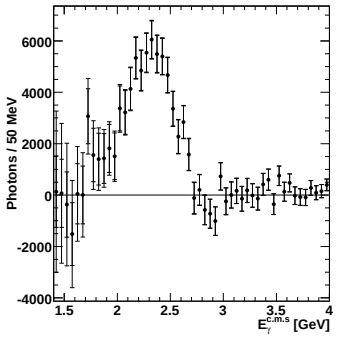

Figure 6. The extracted photon energy spectrum of $B \to X_{s,d}\gamma$. The two error bars show the statistical and total errors.

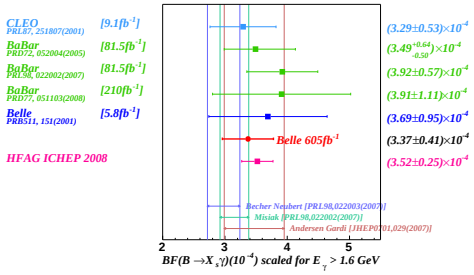

Figure 7. The comparison of experimental results and theoretical predictions. $\mathcal{B}(B \to X_s\gamma)$ is scaled for $E_\gamma^{c.m.s} > 1.6$GeV.

Fig. 7 is the comparison of experimental results and theoretical predictions for the branching fraction. The experimental results are in agreement with the theoretical predictions [7].

4.2. Exclusive $B \to K\eta'\gamma$

We find evidence for $B^+ \to K^+\eta'\gamma$ decays at the 3.3σ level with a partial branching fraction of $(3.2^{+1.2}_{-1.1} \pm 0.3) \times 10^{-6}$. This measurement is restricted to the region of combined $K\eta'$ invariant mass less than 3.4 GeV/c^2. A 90% C.L upper limit of 6.3×10^{-6} is obtained for the decay $B^0 \to K^0_S\eta'\gamma$ in the same $K\eta'$ invariant mass region. Fig.8 shows the distributions of $M_{\rm bc}$ and ΔE with projections from 2D fit results.

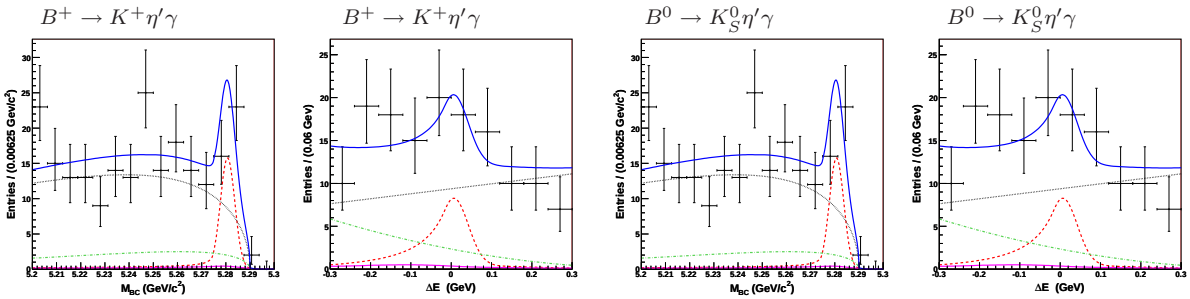

Figure 8. Projections from the 2D fit to data. The $K\eta'\gamma$ function is shown in dashed red, continuum in dotted black, $b \to c$ in dash-dotted green, $b \to u.d.s$ in solid magenta, and th e combined function in solid blue.

5. Summary

We have improved measurements of differential branching fraction, isospin asymmetry, K^* polarization, and forward-backward asymmetry as functions of q^2 for $B \to K^{(*)}ll$ decays and branching fractions for inclusive $B \to X_s\gamma$ and the exclusive $B \to K\eta'\gamma$ modes. There is no evidence so far for new physics. We need much more data sample to improve the sensitivity. Super B-factory will provide one order of magnitude mode luminosity.

[1] G. Buchalla, A. J. Buras and M. E. Lautenbacher, Rev. Mod. Phys. 68, 1125 (1996).
[2] The Belle Collaboration: I. Adachi, *et al.*, arXiv:hep-ex/0810.0335v1(2008).
[3] A. Ali, E. Lunghi, C. Greub and G. Hiller, Phys. Rev. D **66**, 034002 (2002).
[4] The Babar Collaboration: B. Aubert, *et al.*, arXiv:hep-ex/0807.4119(2008).
[5] A. Ishikawa *et al.* (Belle Collaboration), Phys. Rev. Lett. **96**, 251801 (2006); B. Aubert *et al.* (BaBar Collaboration), arXiv:hep-ex/0804.4412v1 (2008).
[6] The Belle Collaboration: I. Adachi, *et al.*, arXiv:hep-ex/0804.1580v1(2008).
[7] M. Misiak *et al.*, Phys. Rev. Lett. **98**, 022002 (2007), For other NNLO calculations, see e.g., T. Becher, M. Neubert, Phys. Rev. Lett. **98**, 022003 (2007), J.R. Andersen, E. Gardi, JHEP 0701:029 (2007).